Published in final edited form as: Molecular and Cellular Endocrinology 473 (2018) 245e256 DOI:10.1016/j.mce.2018.01.025

Hepatic NAD^+ levels and NAMPT abundance are unaffected during prolonged high-fat diet consumption in C57BL/6JBomTac mice

Morten Dall [a], Melanie Penke [b], Karolina Sulek [a], Madlen Matz-Soja [c], Birgitte Holst [d], Antje Garten [b, e], Wieland Kiess [b], Jonas T. Treebak [a, *]

[a] Novo Nordisk Foundation Center for Basic Metabolic Research, Section of Integrative Physiology, University of Copenhagen, Copenhagen, Denmark
[b] Center for Pediatric Research Leipzig, Department for Women and Child Health, University Hospital Leipzig, Leipzig, Germany
[c] Rudolf-Schönheimer-Institute of Biochemistry, Faculty of Medicine, Leipzig University, Leipzig, Germany
[d] Novo Nordisk Foundation Center for Basic Metabolic Research, Section of Metabolic Receptology, University of Copenhagen, Copenhagen, Denmark
[e] Institute for Metabolism and Systems Research, College for Medical and Dental Sciences, University of Birmingham, Birmingham, UK

Abstract

Dietary supplementation of nicotinamide adenine dinucleotide (NAD^+) precursors has been suggested as a treatment for non-alcoholic fatty liver disease and obesity. In the liver, NAD^+ is primarily generated by nicotinamide phosphoribosyltransferase (NAMPT), and hepatic levels of NAMPT and NAD^+ have been reported to be dependent on age and body composition. The aim of the present study was to identify time course-dependent changes in hepatic NAD content and NAD^+ salvage capacity in mice challenged with a high-fat diet (HFD). We fed 7-week-old C57BL/6JBomTac male mice either regular chow or a 60% HFD for 6, 12, 24, and 48 weeks, and we evaluated time course-dependent changes in whole body metabolism, liver steatosis, and abundance of hepatic NAD-associated metabolites and enzymes. Mice fed a 60% HFD rapidly accumulated fat and hepatic triglycerides with associated changes in respiratory exchange ratio (RER) and a disruption of the circadian feeding pattern. The HFD did not alter hepatic NAD^+ levels, but caused a decrease in $NADP^+$ and NADPH levels. Decreased $NADP^+$ content was not accompanied by alterations in NAD kinase (NADK) abundance in HFD-fed mice, but NADK levels increased with age regardless of diet. NAMPT protein abundance did not change with age or diet. HFD consumption caused a severe decrease in protein lysine malonylation after six weeks, which persisted throughout the experiment. This decrease was not associated with changes in SIRT5 abundance. In conclusion, hepatic NAD^+ salvage capacity is resistant to long-term HFD feeding, and hepatic lipid accumulation does not compromise the hepatic NAD^+ pool in HFD-challenged C57BL/6JBomTac male mice

.

1. Introduction

In non-alcoholic fatty liver disease (NAFLD) lipids accumulate in the liver without significant alcohol consumption or viral infection (Angulo, 2002). Reported prevalence varies both with geographic location and detection method applied for diagnosis. Prevalence in the adult European populations ranges from 20% to 31% (Blachier et al., 2013). NAFLD development associates with obesity and type 2 diabetes, where prevalence is reported to be as high as 70% (Lazo and Clark, 2008). As the number of obese people is increasing worldwide, it is estimated that the number of people with NAFLD will follow (Loomba and Sanyal, 2013). While hepatic steatosis has been described as benign and non-progressive (Yilmaz, 2012), several studies have reported progression of NAFLD to non- alcoholic steatohepatitis (NASH) and fibrosis (McPherson et al., 2015; Pais et al., 2013; Wong et al., 2010). NASH can further prog- ress to cirrhosis and liver cancer (Ekstedt et al., 2006). Simple steatosis can be improved through lifestyle intervention (Shah et al., 2009), but boosting levels of nicotinamide adenine dinucle-
otide (NAD^+) has also been suggested as a possible treatment strategy (Gariani et al., 2016).

In the liver, NAD^+ can be generated from tryptophan or nicotinic acid (Fukuwatari and Shibata, 2013), but the majority of NAD^+ is generated from nicotinamide, which is converted to nicotinamide mononucleotide (NMN) in the rate-limiting step mediated by nicotinamide phosphoribosyltransferase (NAMPT), and into NAD^+ by nicotinamide mononucleotide adenylyltransferases (NMNAT1-
3) (Verdin, 2015). In rodents, several studies have demonstrated decreased NAD^+ levels and/or NAMPT abundance in the liver following high-fat diet (HFD) feeding (Choi et al., 2013; Gariani et al., 2016; Uddin et al., 2017; Wang et al., 2017; Yoshino et al., 2011; Zhang et al., 2014; Zhou et al., 2016). NMN can attenuate HFD-induced phenotypes and restore NAD^+ levels (Yoshino et al., 2011). In several other animal models for obesity, dietary supple- mentation with nicotinamide riboside (NR), another NAD^+ pre-cursor, prevented hepatic lipid accumulation, enhanced insulin sensitivity, glucose tolerance, and decreased fat mass accumulation (Canto et al., 2012; Gariani et al., 2016; Trammell et al., 2016). Additionally, supplementation with NAD^+ precursors has been shown to have substantial anti-aging effects in rodents (Mills et al., 2016; Zhang et al., 2016). NAD^+ precursor supplementation is thought to reverse HFD-induced hepatic lipid accumulation through activation of the sirtuins, a family of deacylase proteins (i.e., SIRT1-7). Sirtuins cleave NAD^+ to nicotinamide and O-acetyl- ADP-ribose and activity can be enhanced by increasing NAD^+ levels (Wood et al., 2004). Sirtuins modulate a number of target proteins that regulate glucose and lipid metabolism, mitochondrial function, and mitochondrial biogenesis (Giblin et al., 2014). Decreased he- patic expression of SIRT1, SIRT3, SIRT5, and SIRT6 has been reported in patients with NAFLD (Wu et al., 2014), while liver-specific knockout of SIRT1 and SIRT6 in mice results in hepatic lipid accu- mulation (Kim et al., 2010; Purushotham et al., 2009). Consistently, overexpression of SIRT1 protects against HFD-induced obesity (Pfluger et al., 2008), and increasing the hepatic NAD pool by in- hibition of the NAD^+-consuming enzymes poly-ADP ribose poly- merases (PARPs) decreases weight gain and hepatic steatosis development by a SIRT1-dependent mechanism in high-fat high- sucrose-fed mice (Gariani et al., 2017). Hence, sufficient sirtuin activity appears important for prevention of hepatic lipid accu- mulation. It is not known if impaired NAD^+ synthesis or increased NAD^+ consumption is responsible for diet-induced impairments in sirtuin activity. Furthermore, it is not known if insufficient NAD^+ levels and sirtuin activity precede steatosis development in obese rodents, or if NAD^+ depletion arises following hepatic lipid accu- mulation. In this study, we aimed to determine the HFD-induced and time course-dependent changes in hepatic NAD and NAD^+ salvage systems.

2. Materials and methods

2.1. Chemicals and reagents

Unless otherwise noted, all chemicals and reagents were pur- chased from Sigma Aldrich (Germany).

2.2. Mouse experiments

* Corresponding author. Novo Nordisk Foundation Center for Basic Metabolic Research, Section of Integrative Physiology, Faculty of Health and Medical Sciences, University of Copenhagen, Blegdamsvej 3B, 7.7.46, DK2200 Copenhagen, Denmark.

E-mail address: jttreebak@sund.ku.dk (J.T. Treebak).

Mouse experiments were performed in accordance with the European directive 2010/63/EU of the European Parliament and of the Council for the protection of animals used for scientific pur- poses. Ethical approval was given by the Danish Animal Experi- ments Inspectorate (#2012-15-2934-307).

2.3. *High-fat diet time course experiment*

Sixty-eight male C57BL/6JBomTac (Taconic, Denmark) mice were acquired at 5 weeks of age and were acclimatized to the an- imal facility at University of Copenhagen for 2 weeks. The C57BL/6JBomTac strain was chosen, as these mice do not contain a re- ported mutation in the nicotinamide nucleotide transhydrogenase (NNT) gene known to be present in C57BL/6J mice (Toye et al., 2005). Mice were single-housed and distributed into eight groups, matched by lean body mass determined by NMR scanning (EchoMRI 4-1, EchoMRI, TX, USA). Half of the groups were fed a standard "Chow" diet (Altromin 1319, Brogaarden, Denmark) con- taining 13.7 kJ/g, and the other half was fed a 60% HFD containing 21.8 kJ/g (D12492, Research Diets, NJ, USA). Mice were housed in temperature-controlled conditions (22 ± 1 °C) with a 12-h light/ dark cycle (from 6 AM to 6 PM) and feed and water ad libitum. NMR scanning was used to determine fat mass accumulation and body composition throughout the experiment. For each diet, separate groups were sacrificed at 6, 12, 24, and 48 weeks of treatment after being subjected to one week of metabolic chamber measurements. Mice were given 2 days of recovery after the metabolic chamber measurements before being sacrificed from 1 PM to 5 PM. Mice were sedated using isoflurane and sacrificed by cardiac puncture. The liver was removed and part of the lobus dexter, lobus sinister, and lobus caudatus were fixed in 4% PFA solution. Another part of the lobus dexter and lobus sinister were snap-frozen whole in liquid nitrogen for Oil-Red O staining, and the remaining part of the liver was quickly cut into smaller pieces and snap-frozen in liquid nitrogen. Samples were stored at -80 °C and pulverized in liquid nitrogen prior to analysis.

2.4. *Metabolic chamber measurements*

Prior to the measurements, mice were placed in habituation cages for 6 days, to adapt to the novel environment. Immediately before being transferred to the habituation cages, mice were fasted for 6 h from 8 AM (2 h in light phase), and blood glucose levels were measured from the tail vein (Contour Classic glucose meter; Ascensia Diabetes Care Holdings, Switzerland). Following habitua- tion, mice were placed in the metabolic chambers for one week (TSE LabMaster, TSE Systems, Germany). Oxygen consumption, CO_2 production, food intake, and water intake were evaluated every 20 min. Data from 4 days of measurement were used to calculate average values for each time point for each mouse. These values were then used to calculate the average values for each diet/age group for each time point throughout the light and dark phase.

2.5. *Histology and oil-red o staining*

Frozen liver tissues were cryo-sectioned (6 µm) and stained with Oil-red O for quantitative and qualitative lipid analysis. Liver sections were fixed in 4% PFA, embedded in paraffin, cut in 6 µm slices and stained with hematoxylin/eosin (H&E) (Gebhardt, 1992). For visualization, a Leica DM5000B microscope (Germany) was used.

2.6. *NAD^+, $NADP^+$, NADH, and NADPH measurement*

NAD^+ and NADH levels were determined using an enzymatic cycling assay (Graeff and Lee, 2002). Livers were processed by lysing 10e20 mg of pulverized tissue in 400 mL of either 0.6 M perchloric acid (for NAD^+) or 0.1 M NaOH (for NADH) with a Tis- suelyser II (Qiagen, Hilden, Germany). The NADH extract was incubated at 70 °C for 10 min, and both fractions were centrifuged for 3 min at 13.000 *g*. The supernatants were transferred to new tubes. The NAD^+ extracts were diluted 1:1600 in 100 mM Na_2HPO_4 buffer (pH 8) and the NADH extracts were diluted in 1:500 in 10 mM Tris (pH 6). 100 mL of the diluted extracts were pipetted into a white 96-well plate, and were added 100 mL reaction mix, con- taining 100 mM Na_2HPO_4, 10 mM flavinmononucleotide, 2% ethanol,90 U/mL alcohol dehydrogenase, 130 mU/mL diaphorase, 2.5 mg/mL resazurin and 10 mM nicotinamide. Fluorescence increase (Ex 540 nm/Em 580) was measured over 30 min and content of each metabolite was calculated from a standard curve and normalized to tissue weight. $NADP^+$ and NADPH levels were determined from the same extracts, but with a reaction mix containing 100 mM Na_2HPO_4, 10 mM flavinmononucleotide, 1.2 U/mL glucose 6- phosphate dehydrogenase, 10 mM glucose 6-phosphate, 130 mU/ mL diaphorase, 2.5 mg/mL resazurin and 10 mM nicotinamide.

2.7. *Metabolomics*

Chemicals and reagents: All chemicals and reagents used were of liquid chromatography-mass spectrometry (LC-MS) grade unless otherwise stated. D5-tryptophan, methanol, water, acetonitrile, 2- propanol, formic acid, ammonium hydroxide were purchased from Sigma Aldrich (Denmark) and hexakis(2,2-difluoroethoxy) phosphazene from Apollo Scientific (UK).

Metabolites extraction: Samples were randomized for processing and blanks (empty microcentrifuge tubes) were included in the preparation. Tissues were prepared for metabolomics by weighing off approximately 50 mg of pulverized liver (exact weight was recorded). Each sample was added 0.5 mL cold 50% methanol in water (containing 0.008 mg/mL D5-tryptophan for normalization) and were homogenized using a Tissuelyser II with methanol-washed beads. Each sample was added 0.5 mL chloroform (con- taining 0.013 mg/mL D35 stearic acid for normalization). Samples were vortexed and incubated for 30 min at 1 °C at highest speed on a Thermomixer Comfort (Eppendorf, Germany). Samples were centrifuged at 0 °C for 10 min at 1,500 *g*. Methanol/water fraction was separated from the chloroform one into new pre-chilled tubes. Methanol/water extract was centrifuged at 0 °C for 10 min at 13,400 *g*. Supernatants were transferred to new tubes and after short vortexing 10 mL of each sample was collected to one pre- chilled microcentrifuge tube, creating a Quality Control sample (QC). Finally, all samples were stored at -80 °C until LC-MS analysis.

LC-MS metabolic profiling: Methanol/water extracts, QC samples and blanks were defrosted on ice, vortexed and set in a pre-chilled LC-MS vial (Verex Vial, mVial i3 Qsert, Phenomenex) with a screw- cap (Verex Cert + MSQ Cap, Phenomenex). Leftover samples were stored at -80 °C. Metabolic profiling was conducted using a LC-MS system: Samples were maintained at 4 °C throughout the analysis. QC samples and blanks were injected after each 5th sample. Chromatographic separation was performed using UHPLC Dionex Ultimate 3000 (Thermo Scientific, Germany) with Luna Polar C18 column (1.6 mm, 2.1 x 100 mm, Phenomenex, USA) with EVO C18 guard column (sub-2mm, 2.1 mm, Phenomenex, USA) kept at 40 °C. Solvent A and B were 0.1% formic acid in acetonitrile and 0.1% formic acid with 5 mM ammonium hydroxide in LC-MS grade water, respectively. A flow rate of 0.3 mL/min was applied with a gradient elution profile: 95% B 0e1 min, 95%e5% B 1.0e10.0 min, 5% B 10.0e12.0 min, 5e95% B 12.0e12.5 min, 95% B 12.5-14-5 min (equilibration step). LC was coupled with QToF Impact II mass spectrometer (Bruker Daltonics, Germany) operating in electro- spray ionization. Samples were analyzed in positive and negative mode. 5 mL of the extract was injected in positive mode and 10 mL in the negative mode. Line and profile MS spectra were acquired in the mass range 50e1000 mass to charge ratio (m/z) at 2.00 Hz spectra rate using the source settings for positive mode: absolute threshold 50 cts per 1000 sum, End Plate Offset 500 V, Capillary 4500 V, Nebulizer 2.0 Bar, Dry Gas 10.0 l/min, Dry Temperature 220 °C; Transfer: Funnel 1RF 150.0 Vpp, Funnel 2FR 200.0 Vpp, isCID Eergy 0.0 eV, Hexapole RF 50.0Vpp; Quadrupole: Ion Enegry 4.0 eV, Low Mass 100.0 m/z; Collision Cell: Collision Energy 7.0 eV, Transfer Time 65.0 ms, Collision RF 650.0 Vpp, Pre Pulse Storage 5.0 ms. In negative mode Capillary voltage was set to 3000 and other pa- rameters were identical as described above for both modes. MS spectra were divided into 3 segments: pre-analysis 0e0.1 min, calibration 0.1e0.5 min, analysis 0.5e14.5 min. External and inter- nal calibration was based on sodium formate clusters in 2-propanol with Zoom of 1.0% and HPC mode. Additionally, lock-mass cali- bration based on hexakis(2,2-difluoroethoxy)phosphazene in 2- propanol (0.1 mg/mL) throughout the whole scan was applied. Targeted MSMS analysis

Published in final edited form as: Molecular and Cellular Endocrinology 473 (2018) 245e256 DOI:10.1016/j.mce.2018.01.025

was performed at the same LC-MS settings as the MS scans with additional collision energy set to 20 and scan width 1.0 m/z for both negative and positive mode.

LC-MS data analysis: Raw data from the positive and negative mode were automatically calibrated according to the sodium- clusters and lock-mass shifts throughout the analysis, using the Compass Data Analysis 4.3 (Bruker Daltonics, Germany). Files were converted to NetCDF format through the Bruker software and metabolic features were extracted using R-based (Team, 2013) XCMS (Smith et al., 2006), following CAMERA analysis (Kuhl et al., 2012). Data were normalized according to the internal standard abundance and samples weight. Statistical analysis was performed using online analytical tools within MetaboAnalyst 3.0 (Xia and Wishart, 2002). CAMERA-generated buckets were log- transformed and Pareto-scaled. Non-informative variables were removed based on their standard deviation. Initially Principal Component Analysis was made to visualize the clustering of the samples, QCs and blanks in search for potential contaminations, machine drifts and outliers. Two-factor independent study using 2- way ANOVA with False Discovery Rate (FDR) analysis was used to select significantly different metabolic features. Initially, signifi- cantly different metabolic features ($p < 0.05$, FDR corrected) were matched with metabolites in Human Metabolome Database (Wishart et al., 2013) and Metlin Database (Smith et al., 2005) ac- cording to the mass to charge ratio. Provided at the databases ID numbers for metabolites in Kyoto Encyclopedia of Genes and Ge- nomes (KEGG) (Kanehisa et al., 2017) were used to perform a batch search in relation to affected pathways. Following, MSMS profile was acquired for metabolites from significantly affected metabolic pathways and matched to the MSMS from databases.

2.8. Western blot analyses

For Western blot analyses, approximately 20 mg pulverized tissue was homogenized in 500 mL lysis buffer (pH 7.4, 10% glycerol, 1% IGEPAL, 50 mM Hepes, 150 mM NaCl, 10 mM NaF, 1 mM EDTA, 1 mM EGTA, 20 mM sodium pyrophosphate, 2 mM sodium ortho-vanadate, 1 mM sodium-pyrophosphate, 5 mM nicotinamide, 4 mM Thiamet G and protease inhibitors (S8820, SigmaFast)) using a Tissuelyser II (Qiagen, Germany), 2 x 30 s of 30 Hz. Lysates were incubated end-over-end for 45 min at 4 °C, and were centrifuged for 10 min at 16.000 *g* at 4 °C. Protein concentration was deter- mined using the Bicinchoninic Acid Assay (23227, ThermoFisher Scientific, MA, USA). 20 mg of protein lysate was loaded on acryl- amide SDS-page gels and subject to electrophoresis, together with Precision Plus Protein All Blue Standards and Precision Plus Protein Dual Color Standards (Bio-Rad, CA, USA) to determine band size. Proteins were then transferred to polyvinyl difluoride membrane (PVDF, #Ipvh00010, Millipore, Germany) by semi-dry transfer and subjected to immunoblotting. Membranes were incubated ac- cording to the manufacturer's instructions with the following an- tibodies: NAMPT (372A, Bethyl lab, TX, USA), NMNAT1 (45548, Abcam, UK), NMNAT3 (116288, Abcam), NRK1 (398852, Santa Cruz, TX, USA), AFMID (19522-1-AP, Proteintech, IL, USA), NAPRT1 (123023, Abcam), NADK (A304-993A, Bethyl Labs), SIRT1 (07-131, Millipore), SIRT3 (5490, Cell Signaling, MA, USA), SIRT5 (8782, Cell signaling), SIRT6 (12486, Cell Signaling), PARP1 (9542, Cell Signaling), Acetyl Lysine (9441s, Cell Signaling), Malonyl Lysine (14942, Cell Signaling). Following wash in TBS-T, membranes were incubated with HRP-conjugated antibodies, anti-rabbit (170-6515, Biorad, CA, USA) or anti-mouse (170-6516, Biorad) according to the manufacturer's instructions. Membranes were developed using a Chemidoc XRS+ (Biorad) using Lumina Forte Western HRP Substrate (Millipore). Bands were quantified using the Image Lab software (Bio-Rad) and band intensity was normalized to the band intensity of an internal control of mixed liver samples loaded twice on all gels.

2.9. Quantitative real-time PCR

Total RNA of liver tissue was extracted by TRIzol® Reagent (Life Technologies) according to manufacturer's protocol. 1 mg of total RNA was transcribed into cDNA by M-MLV Reverse Transcriptase (#28025013, Invitrogen). Quantitative PCR analyses were per- formed using the qPCR Master Mix Plus Low ROX (Eurogentec) or Absolute qPCR SYBR Green Low ROX Mix (Thermo Scientific) and the Applied Biosystems 7500 Real Time PCR System. *Nampt* mRNA expression (forward: 5^0- GAT GGT CTG GAA TAC AAG TTA CAT GAC T-3'; reverse: 5^0-ATG AGC AGA TGC CCC TAT GC-3^0, probe: 5^0-AGG AGT CTC TTC GCA AGA GAC TGC T-3^0) was normalized to Cyclo- phillin (forward: 5^0- ATG TGG TTT TCG GCA AAG TT-3'; reverse: 5^0- TGA CAT CCT TCA GTG GCT TG-3^0)

2.10. Statistical analysis

Data are presented as mean ± SEM. Data were analyzed using 2- way analysis of variance (ANOVA) with Sidak's multiple compari- son test post hoc. All statistical analysis was performed using Graphpad Prism 6 (Graphpad Software, CA, USA). Statistical sig- nificance was defined as $p < 0.05$. */** indicate effects of diet, $p < 0.5/0.01$, respectively. #/## indicate effects of age, $p < 0.05/0.01$, respectively.

3. Results

3.1. Six weeks of high-fat diet causes fat mass accumulation, decreased RER, and altered feeding behavior

We first investigated how HFD feeding affects fat mass accu- mulation and whole-body metabolism over time. While no change was observed in absolute weight between chow- and HFD-fed mice until week 36 (Fig. 1A, $p < 0.01$, $n = 8$), there was a marked differ- ence in body composition early after HFD exposure. In HFD-fed mice, weight gain was due to rapid fat mass accumulation, which kept increasing throughout the study (Fig. 1B, $p < 0.01$, $n = 7e8$). In contrast, during the first 12 weeks chow-fed mice showed a larger increase in lean mass gain compared to the HFD group, which persisted throughout the study (Fig. 1C, $p < 0.01$, $n = 7e8$). 6 weeks of HFD feeding caused major changes in RER and feed intake pat- terns. Throughout the study, a circadian pattern in RER was observed in chow-fed mice, with a large increase in RER during the dark phase, which became smaller with age (Fig. 1D). The HFD-fed mice had only minor circadian RER oscillations at all 4 time-points. Daily food intake patterns were only different between diets at 6 and 12 weeks, where a significant interaction was observed be- tween diet and time of day (Fig. 1E). At the first two time-points, chow-fed mice were primarily eating in the dark phase, while HFD-fed mice had a continuous food intake throughout the dark and light phase. The chow group's feeding pattern became more irregular after 24 weeks (diet x feeding time interaction effect, $p = 0.07$), and after 48 weeks mice consumed an equal amount of calories throughout dark and light phase regardless of diet. Hence, HFD consumption caused major changes in whole-body meta- bolism within the first 6 weeks of the study. Fasting blood glucose levels were not affected by age, and did not differ between chow- and HFD-fed mice (Fig. 1F). Thus, HFD consumption caused major changes in whole-body metabolism in C57BL6/JBomTac mice within the first 6 weeks of HFD feeding, but glycemic control did not appear to be affected by the dietary intervention.

3.2. High-fat diet feeding causes progressive accumulation of hepatic triglycerides

To assess if liver steatosis development accompanied the rapidly induced HFD phenotype, we measured hepatic triglyceride content by oil-red o staining (Fig. 2A). HFD feeding caused a significant increase in hepatic lipid content after 6 weeks, which became more severe with time (Fig. 2C, $p < 0.01$, $n = 3$). The presence of steatosis in the HFD-fed groups was also confirmed by H&E staining, which showed visible steatosis after 24 weeks (Fig. 2B). After 48 weeks, chow-fed mice also had an increased content of lipids compared to earlier time points (Fig. 2C, $p < 0.01$, $n = 3$). Therefore, while HFD causes rapid accumulation of hepatic lipids, this did not progress to macrovesicular steatosis until after 24 weeks. Hence, whole-body fat mass accumulation preceded hepatic macrovesicular steatosis.

3.3. High-fat diet feeding decreases hepatic NADP(H) content but not NAD^+ levels

To assess if hepatic NAD levels were affected by HFD-induced hepatic lipid accumulation, we measured hepatic NAD^+, NADH, $NADP^+$, and NADPH content at all 4 time-points. Hepatic NAD^+ levels were not significantly altered by HFD feeding, but were decreased in the 48-week groups compared to the 24-week groups (Fig. 3A, $P < 0.05$, $n = 7$-9). NADH levels were not significantly altered, though we observed borderline effects of both age ($p ¼ 0.06$) and diet ($p ¼ 0.09$) (Fig. 3B, $n = 7$-9). In contrast, we observed a small, but consistent decrease in NADP levels in all the HFD groups (Fig. 3C, $p < 0.01$, $n = 7$-9). The same was observed for NADPH (Fig. 3D, $p < 0.01$, $n = 7$-9). LCMS analysis confirmed the HFD-induced decrease in $NADP^+$ (data not shown) but no other terms associated with NAD metabolism were altered with age or diet. Enrichment analysis of the metabolomics data suggested changes in purine metabolism. As generation of NAD^+ and NADP requires ATP (Canto et al., 2015), we quantified levels of ATP- associated metabolites in the liver samples. Hepatic ATP levels increased during the first 24 weeks of the experiment and decreased after 48 weeks regardless of diet (Fig. 3E, $p < 0.01$). Levels of adenine, a pre-cursor of ATP (Dudzinska et al., 2010), decreased slightly with age (Fig. 3F, $p < 0.05$), and levels of hypoxanthine, a deamination product of AMP, likewise decreased from 6 to 24 weeks (Fig. 3G, $p < 0.01$). This indicates decreased purine catabo- lism with age (Maiuolo et al., 2016) that may have caused the in- crease in hepatic ATP levels. No change was observed for AMP levels with age, but AMP levels were increased in HFD-fed groups (Fig. 3H). Adenosine levels oscillated slightly with age (Fig. 3I, main effect of age $p < 0.05$), with a borderline increases after 12 weeks ($p = 0.07$) which decreased after 48 weeks ($p = 0.07$). We observed no enrichment for terms associated with the pentose phosphate pathways with age or diet (data not shown), suggesting no change in levels or synthesis of phosphoribosyl pyrophosphate, the co- substrate of NAMPT. However, our analysis revealed a significant decline in nicotinamide content from 6 to 12 weeks regardless of diet (Fig. 3I, $p < 0.05$), which persisted throughout the experiment. While there was no significant difference between the 6-week and 48-week groups, we still observed a tendency towards a decrease

Published in final edited form as: Molecular and Cellular Endocrinology 473 (2018) 245e256 DOI:10.1016/j.mce.2018.01.025

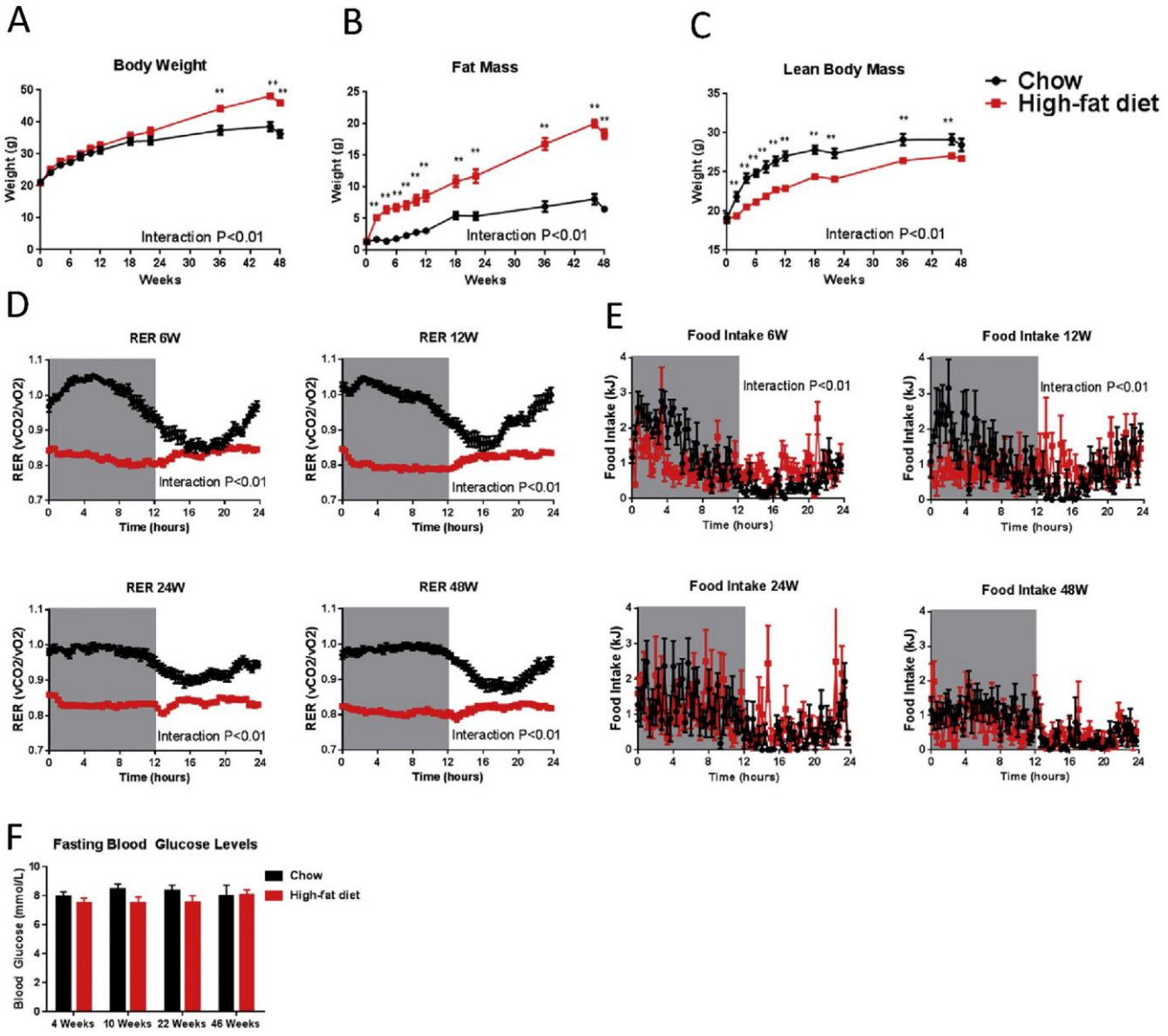

Fig. 1. High-fat diet feeding causes mice to rapidly accumulate fat mass, decrease RER and affect their circadian feeding pattern. Mice were fed a 60% HFD for 48 weeks. Throughout the experiment, (A) total body weight, (B) fat mass, and (C) lean mass were measured. Prior to each sacrifice point, mice were monitored in metabolic chambers. Graphs show pooled averages for the first 4 days of measurements. Grey area indicates dark phase and white area indicates light phase. Graphs show (D) average RER and (E) Food intake in kJ, after 6, 12, 24, and 48 weeks of either chow (black) or HFD consumption (red). */** indicate effects of diet, $p < 0.5/0.01$, respectively. #/## indicate effects of age, $p < 0.05/0.01$, respectively. n = 7e8 per group per time point.

($p = 0.08$). This could indicate a decrease in hepatic NAD turnover or an improvement of NAD^+ salvage capability. Thus, the LCMS analysis demonstrated only minor changes in hepatic NAD meta- bolism with age and HFD feeding in C57BL/6JBomTac mice.

3.4. Abundance of NAD^+ consuming or -synthesizing enzymes is resistant to HFD feeding

Aging in mice has been reported to cause a shift in hepatic NAD^+ salvage pathways, with a decreased abundance of NAMPT and an increased abundance of NMNATs and enzymes involved with *de novo* synthesis of NAD (Zhou et al., 2016). As HFD feeding has also been reported to affect mRNA levels of NAD^+ salvage pathway enzymes (Drew et al., 2016), we investigated if protein abundance of these enzymes were altered by age and/or diet. NAMPT protein abundance was not affected by age or diet (Fig. 4A), but *Nampt* mRNA levels increased with age regardless of diet, indicating that more *Nampt* mRNA is required to maintain NAMPT protein abun- dance (Fig. 4B, $p < 0.01$, $n = 8$). NMNAT1 abundance increased after 24 weeks and 48 weeks regardless of diet (Fig. 4C, $p < 0.01$, $n = 7$-9), but was significantly increased in HFD-fed compared to chow-fed animals ($p < 0.05$). In contrast, NMNAT3 abundance was decreased in HFD-fed animals (Fig. 4D, main effect $p < 0.05$, $n = 7$-9) but did not change with age. This could indicate an increased demand for NAD^+ in the nucleus where NMNAT1 is localized, with a corresponding decreased demand for NAD^+ in the mitochondria where NMNAT3 is localized. Nicotinamide riboside kinase 1 (NRK1) abundance was increased after 48 weeks compared to the 6-week time-point (Fig. 4E, $p < 0.01$, $n = 7$-9) but was not affected by diet. Abundance of Arylformamidase (AFMID),

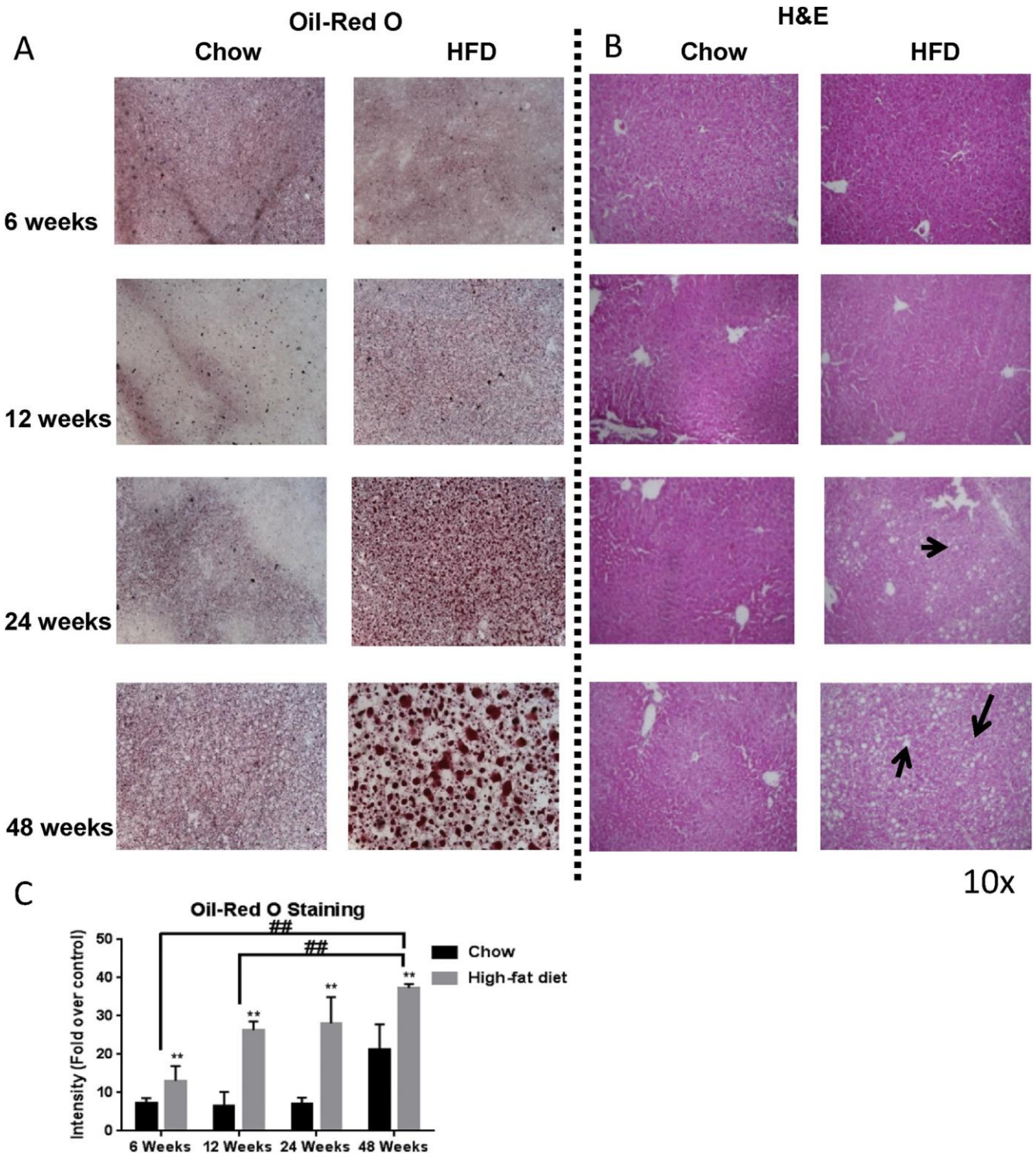

Fig. 2. High-fat diet feeding causes hepatic lipid accumulation. Livers were oil-red o stained to evaluate hepatic lipid accumulation. (A) Representative images for each time-point were selected for the figure. (B) To assess hepatic steatosis development, livers were subject to H&E staining. Representative images from each time point are displayed. (C) Staining intensity of the oil-red O sections was used to quantify hepatic lipid content (n = 3 per group per time point). */** indicate effects of diet, $p < 0.5/0.01$, respectively. #/## indicate effects of age, $p < 0.05/0.01$, respectively.

an essential enzyme in the generation of NAD from tryptophan, was not significantly affected by either diet or age (Fig. 4F). NAPRT1, which converts nicotinic acid to nicotinic acid mononucleotide was not altered by diet or age (Fig. 4G, n = 7-9). As HFD caused a decrease in NADP(H) levels, we measured abundance of NADkinase (NADK) (Verdin, 2015). NADK levels were not affected by HFD, but increased with age in both diet groups (Fig. 4H, $p < 0.01$, n = 7-9). While the abundance of NAD^+ synthesizing enzymes were not dramatically affected by HFD feeding, we hypothesized that NAD^+ consuming enzymes could be affected. HFD feeding or aging did not

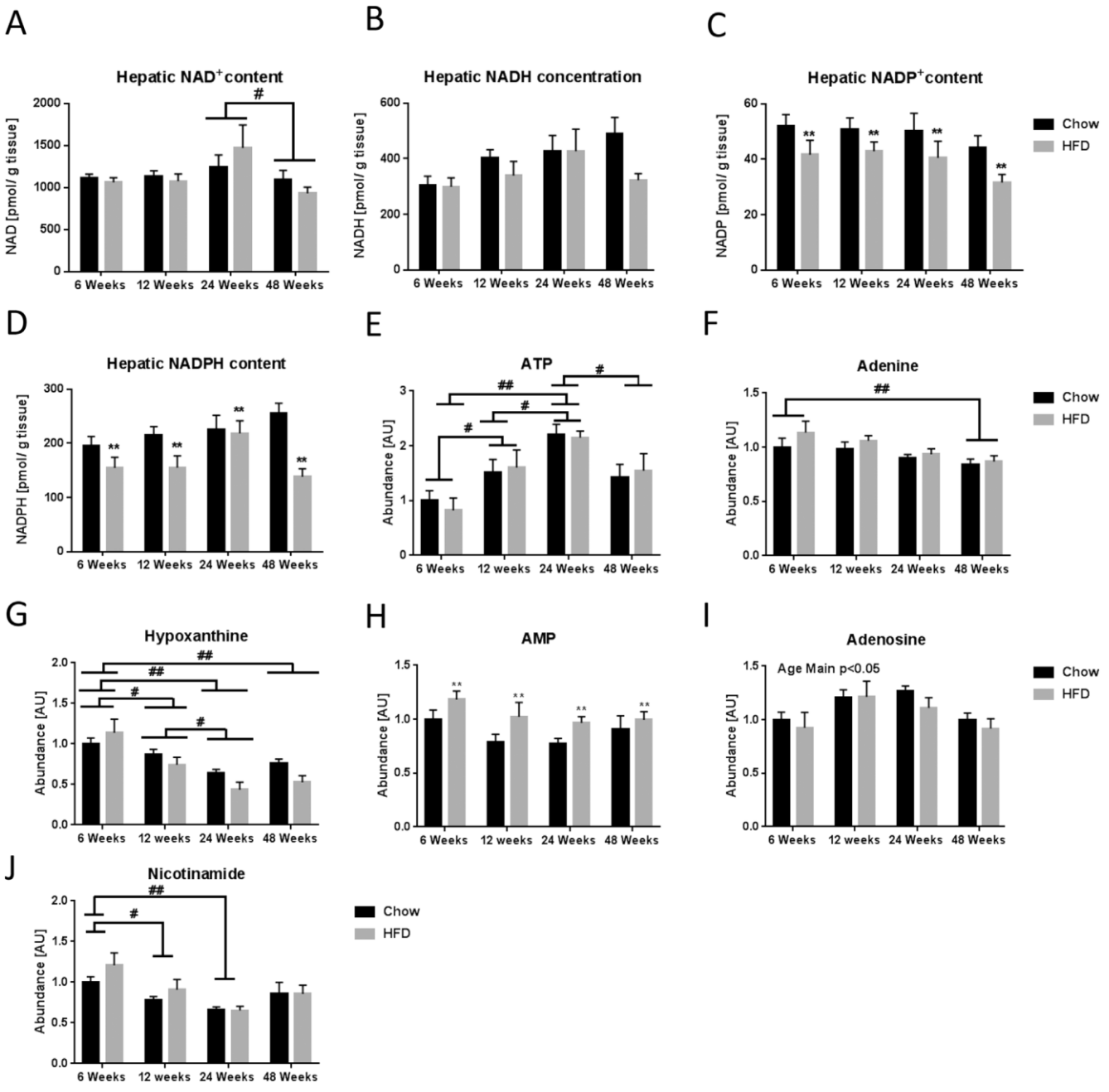

Fig. 3. High-fat diet feeding decreased hepatic NADP and NADPH levels without affecting NAD content. To investigate how high-fat diet feeding affects the hepatic NAD pool, we measured liver (A) NAD^+ levels and (B) NADH levels. We also measured (C) $NADP^+$ levels and (F) NADPH levels. Using MSMS we measured abundance of (D) ATP, (E) Adenine, (F) Hypoxanthine, (G) AMP, (G) Adenosine, and (I) nicotinamide. */** indicate effects of diet, $p < 0.5/0.01$, respectively. #/## indicate effects of age, $p < 0.05/0.01$, respectively. n = 7-9 per group per time point.

affect protein abundance of SIRT1, SIRT3, SIRT5, or SIRT6 (Fig. 4IeL). In contrast, PARP1 abundance was slightly elevated in HFD-fed mice (Fig. 4M, $p < 0.05$, n = 7-9). To evaluate if endogenous sir- tuin activity was altered, we determined two sirtuin-regulated post-translational modifications of lysine residues, acetylation (Fig. 5A) and malonylation (Fig. 5B) (Du et al., 2011; Giblin et al., 2014). A tendency towards decreased acetylation following HFD feeding was observed (Fig. 5A, $p = 0.09$), as was a tendency towards decreased lysine acetylation with age (Fig. 5A, $p = 0.05$). In contrast, HFD-feeding resulted in decreased global lysine malonylation of multiple bands from 6 weeks of HFD-feeding (Fig. 5B, $p < 0.05$). This change persisted throughout the experiment. Hence, while HFD feeding only cause minor changes to NAD-associated metabolites and proteins, lysine malonylation is rapidly affected by HFD consumption.

4. Discussion

The relationship between NAMPT/NAD^+ levels and NAFLD development is incompletely known. Data obtained from humans are inconclusive with one study reporting decreased *NAMPT* mRNA expression in the liver of NAFLD patients compared to healthy controls (Dahl et al., 2010), whereas another study reported increased hepatic *NAMPT* mRNA levels in morbidly obese patients

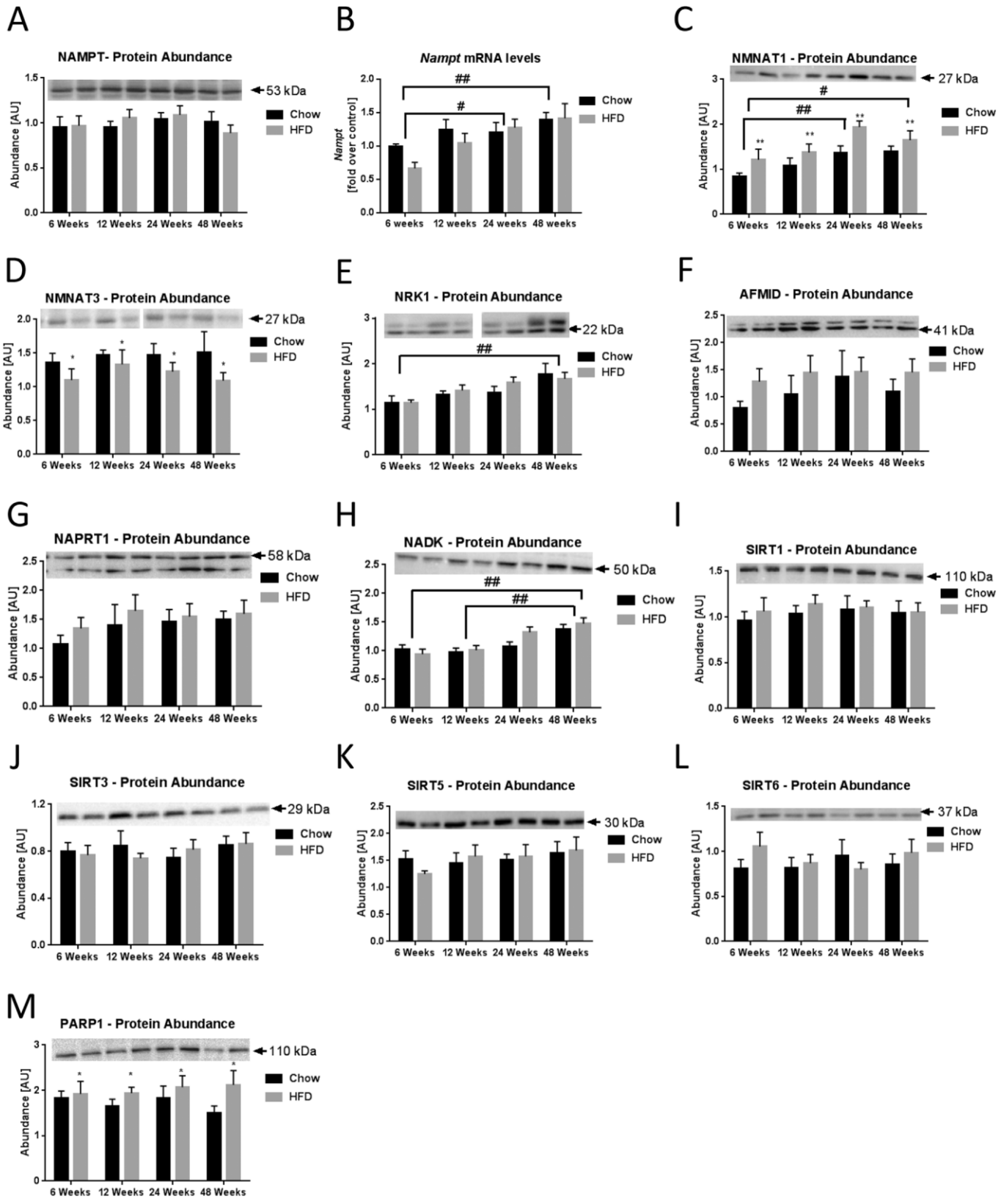

Fig. 4. High-fat diet feeding alters NMNAT abundance but does not significantly affect abundance of NAD^+ synthesizing or NAD^+ consuming enzymes. To investigate how HFD- feeding and aging affected the proteins involved in NAD^+ salvage, we measured hepatic (A) NAMPT protein abundance, (B) *Nampt* mRNA levels, (C) NMNAT1 protein abun- dance, (D) NMNAT3 protein abundance, (E) NRK1 protein abundance, (F) AFMID protein abundance, (G) NAPRT1 protein abundance, and (H) NADK protein abundance. We also measured the abundance of (I) SIRT1, (J) SIRT3, (K) SIRT5, (L) SIRT6, and (M) PARP1. */** indicate effects of diet, $p < 0.5/0.01$, respectively. #/## indicate effects of age, $p < 0.05/0.01$, respectively. n = 7-9 per group per time point.

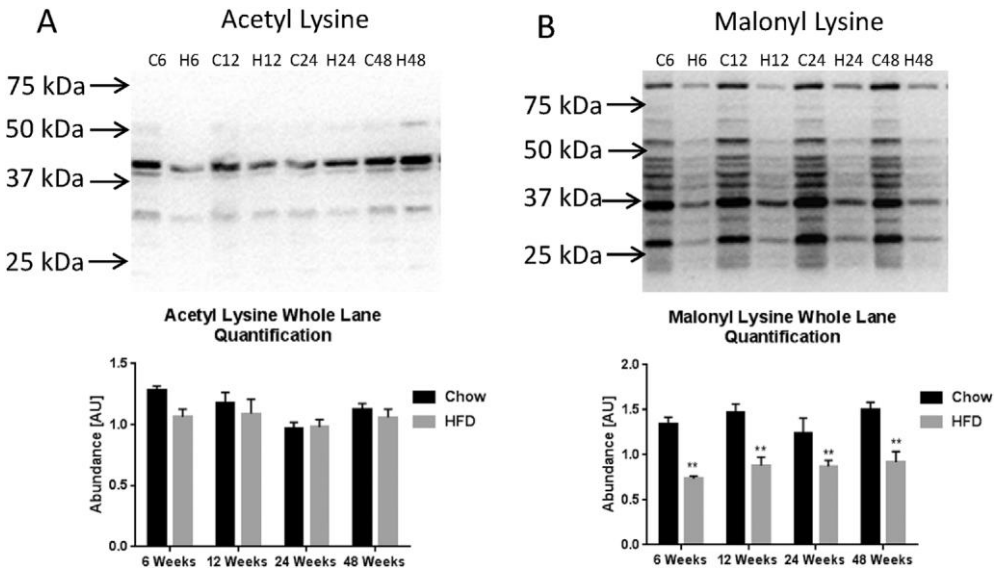

Fig. 5. High-fat diet feeding causes decreased global lysine malonylation. To evaluate how sirtuin-regulated lysine modifications were affected by HFD consumption and aging, (A) global lysine acetylation and (B) global lysine-malonylation were measured by Western blot analyses. Lane intensity was quantified and used to determine effects of age or diet on lysine acetyl/malonylation. */** indicate effects of diet, $p < 0.5/0.01$, respectively. #/## indicate effects of age, $p < 0.05/0.01$, respectively. n = 7-9 per group per time point.

compared to lean controls (Auguet et al., 2013). To understand how obesity and hepatic lipid accumulation affect NAD metabolism and the hepatic NAD^+ salvage pathway, we performed a HFD time course study for 48 weeks in C57BL/6JBomTac mice. While the decreased lean mass in the HFD-fed groups was surprising, the increased fat mass accumulation, changes in RER, and altered feeding behavior are well-characterized effects of HFD feeding (Kohsaka et al., 2007; Williams et al., 2014). We found that mice accumulated a large amount of fat mass and hepatic triglycerides, which was associated with decreased hepatic content of $NADP^+$ and NADPH as previously reported (Trammell et al., 2016). The decreased $NADP^+$ levels were not accompanied by a decrease in NADK abundance. However, NADK abundance increased with age regardless of diet, which may reflect higher demands for NADP with age.

HFD consumption did not severely affect hepatic NAD^+ levels, the abundance of NAD^+ producing enzymes, or sirtuin protein levels. This is in contrast to several previous studies, which have described decreased NAMPT and/or NAD^+ levels in the liver of obese rodents (Choi et al., 2013; Gariani et al., 2016; Uddin et al., 2017; Wang et al., 2017; Yoshino et al., 2011; Zhang et al., 2014; Zhou et al., 2016). Moreover, we have previously reported elevated hepatic NAD^+ levels in HFD-fed mice (Penke et al., 2015), and levels of *Nampt* mRNA were increased and NAD^+ unaltered in mice fed a 60% HFD from 3 days to 16 weeks (Drew et al., 2016). While most of the studies compare HFD-fed animals to animals fed an unmatched chow diet, two studies used a matched low-fat diet to ensure comparable micronutrient composition of the diets (Wang et al., 2017; Zhang et al., 2014). Thus, one explanation for the discrepancies in the reported responses to HFD feeding may be related to the level of NAD^+ precursors in the diets. However, levels of NAD^+ precursors in the diets used in the present study do not appear to explain the inconsistent findings. While none of the diets contained nicotinamide, nicotinic acid content was 63 mg/g diet in chow vs. 30 mg/g diet in the HFD. Moreover, tryptophan levels were 2.9 mg/g diet in the chow diet, but tryptophan content of the HFD was not reported by the manufacturer. Tryptophan content in the HFD can, however, be estimated to 3.2 mg/g, as this diet contained 258.4 g casein pr. kg, with an estimated tryptophan content of 12.5 mg/g protein (Bendtsen et al., 2014).

Differences between studies could result from different methods of assessing NAD^+ content. However, studies obtaining different results have used similar methodologies to determine NAD^+ levels. For instance, commercial kits were used in some studies (Choi et al., 2013; Drew et al., 2016; Wang et al., 2017; Zhou et al., 2016), while other studies used mass spectrometry (Gariani et al., 2016), HPLC (Penke et al., 2015; Yoshino et al., 2011), or a cycling assay (Uddin et al., 2017) similar to the assay applied in the present study. Thus, results appear not to be associated with a particular method for NAD^+ detection.

Differences between observed changes in NAD^+ in response to dietary interventions could potentially be due to the specific mouse strains used and how well glycemic control is maintained. Per- turbed whole body glucose metabolism may affect the hepatic NAD^+ pool more than obesity. For instance, a ~20% decrease in hepatic NAD^+ was observed after 20 weeks of 60% HFD feeding, but this was further reduced to 50% when these mice were treated with streptozotocin to induce diabetes (Trammell et al., 2016). We used C57BL6/JBomTac mice that were able to maintain glycemic control throughout the study. Interestingly, the C57BL6/JBomTac mice have recently been demonstrated to have a deletion in the Y-chromo- some that confers decreased fertility (MacBride et al., 2017). However, whether this deletion plays any role in maintaining NAD^+ levels in C57BL/6JBomTac mice on a HFD has not been investigated. A mutation in the *Nnt gene* in C57BL/6J was demonstrated to contribute to the impaired glucose tolerance observed in this strain (Toye et al., 2005). The majority of studies demonstrating decreased NAD^+ levels in the liver of HFD-fed animals have been conducted in C57BL/6J (Gariani et al., 2016; Uddin et al., 2017; Zhou et al., 2016). Studies reporting no changes or increases in hepatic NAD^+ content after HFD feeding, however, were performed in C57BL/6 mice without the *Nnt* mutation (Drew et al., 2016; Penke et al., 2015; Williams et al., 2014). Thus, it is possible that the mutation in *Nnt* contributes to the decrease in NAD^+ levels in HFD-fed C57BL/6J mice. It should be noted that decreased NAD^+ levels in response to a HFD are not limited to C57BL/6J mice. Decreased NAD^+ levels following HFD have been observed in ICR mice (Wang et al., 2017; Zhang et al., 2014) and BALB/C mice (Choi et al., 2013).

A final source of variation between studies could be time of sacrifice, as NAD^+ levels and *Nampt* mRNA levels oscillate (Ramsey et al., 2009). However, as most reports do not state the time of sacrifice, it is not possible to assess if time of sacrifice is an important factor in this context.

NAMPT protein abundance in the liver was unaffected by HFD consumption in our study. In contrast to NAMPT, NMNAT1 abundance was slightly increased in HFD-fed mice, and NMNAT3 abundance was decreased. Another study reported increased *Nmnat1* mRNA levels and decreased NMNAT3 protein abundance in the first week of HFD feeding, but this was normalized after 3 weeks (Drew et al., 2016). NMNAT1 levels generally increased with age, which was also the case for NRK1. NRK1 is essential in processing NR, but is also important for utilizing NMN (Ratajczak
et al., 2016). The increased abundance of these two enzymes may suggest an increased demand for NAD^+ with age. PARP1 abundance increased slightly with HFD, which was also previously observed for mRNA levels (Drew et al., 2016). On the other hand, none of the investigated sirtuins changed in abundance with age
or diet. Thus, while hepatic knockout of SIRT1 and SIRT6 causes steatosis (Kim et al., 2010; Purushotham et al., 2009), HFD-induced hepatic steatosis *per se* does not affect the abundance of these proteins. We cannot rule out that endogenous sirtuin activity is affected, as mice fed a 45% HFD for 16 weeks had decreased hepatic SIRT3 activity, but unaltered SIRT3 abundance (Kendrick et al., 2011). The effects of HDF feeding on hepatic SIRT3 abundance is unclear, as another study reported decreased SIRT3 abundance after HFD feeding (Hirschey et al., 2011). This study also reported hepatic hyperacetylation following chronic HFD feeding, which was not observed in our study. In contrast, malonyl-lysine band intensity was reduced in HFD-fed mice after
6 weeks, which persisted throughout the experiment. Lysine residues are demalonylated by SIRT5 (Du et al., 2011), but SIRT5 abundance was unaltered between chow-fed and HFD-fed mice in our study, indicating either increased SIRT5 activity or decreased addition of malonyl to lysine targets. SIRT5 regulates a range of important processes in the liver, such as the urea cycle, ketogenesis and b-oxidation. Mice fed a 60% HFD for 16 weeks have increased malonyl-CoA levels compared to LFD-fed mice (Go et al., 2016), which could suggest that malonyl-CoA accumulates, even though altered malonyl-CoA levels were not observed in our LCMS analysis. Malonyl-CoA is an important metabolite for regulating fatty-acid oxidation and synthesis (Saggerson, 2008). A previous study investigated the malonylome by proteomic analysis, and found that 72% of the identified malonylated proteins were involved in metabolism, especially glucose metabolism (Du et al., 2015). It is currently not known how malonylation affects protein activity, although site-specific malonylation of fructose bisphosphate aldolase B (ALDOB) decrease the enzymatic activity (Du et al., 2015). Decreased protein malonylation may therefore represent an early adaptation to a fat-based metabolism. However, the significance of malonylation for adapting to HFD-feeding remains undetermined.

In conclusion, we find that hepatic lipid accumulation in response to prolonged HFD feeding in C57BL/6JBomTac mice does not affect the hepatic NAD^+ pool or compromise the hepatic NAD^+ salvage pathway. While HFD causes major changes to whole body metabolism, the liver NAD^+ salvage system is resilient, even in the presence of macrovesicular steatosis. HFD causes minor changes in the abundance of NMNAT1, NMNAT3, PARP1, $NADP^+$, and NADPH, but not NAMPT or NAD^+. As HFD feeding *per se* does not appear to affect the function of the NAD^+ salvage pathway, the decreased NAD^+ salvage pathway function reported in other studies could be mediated by other factors than hepatic lipid accumulation.

Funding

This work was funded in part by grants obtained by JTT from the Novo Nordisk Foundation (Excellence Project Award, NNF14OC0009315), and the Danish Council for Independent Research (DFF 4004-00235). Moreover, support for this study was also provided by the Novo Nordisk Foundation Center for Basic Metabolic Research (NNF-CBMR). NNF-CBMR is an independent Research Center at the University of Copenhagen and partially funded by an unrestricted donation from the Novo Nordisk Foundation, (http://metabol.ku.dk). MD was supported by a 1/3 PhD stipend from the Danish Diabetes Academy, funded by the Novo Nordisk Foundation. Support for this project was also provided by the European Foundation for the Study of Diabetes (EFSD) Albert Renold Travel Fellowship Programme (to MP), and from the European Union's Horizon 2020 research and innovation programme under the Marie Sklodowska-Curie grant agreement No 705869 (to AG).

Author contribution

JTT, WK, MP, AG and MD conceived the study. JTT, MP and MD designed the study. All sample collection and processing was done by MD and MP. BH provided scientific and technical support for the metabolic chamber measurements. KS performed the LCMS and MSMS data collection and analysis. MP and MMS performed histology and oil-red O analysis. MD analyzed all additional data. MD, AG, MP and JTT interpreted the data. MD and JTT wrote the manuscript, which was critically revised and accepted by all authors. JTT is the guarantor of this work, has full access to all the data in the study, and takes responsibility for the integrity of the data and the accuracy of the data analysis.

Conflicts of interest

The authors declare no conflict of interest in relation to this work.

Acknowledgements

The authors acknowledge the skilled technical assistance provided by Steve Risis, Søren Madsen, and Andreas Nygaard Madsen from the Novo Nordisk Foundation Center for Basic Metabolic Research, University of Copenhagen, by Doris Mahn from the
Rudolf-Schönheimer-Institute of Biochemistry, University of Leipzig, and by Anja Barnikol-Oettler and Sandy Richter from the Center for Pediatric Research, University Children's Hospital Leipzig.

References

Angulo, P., 2002. Nonalcoholic fatty liver disease. N. Engl. J. Med. 346, 1221e1231. Auguet, T., Terra, X., Porras, J.A., Orellana-Gavaldà, J.M., Martinez, S., Aguilar, C., Lucas, A., Pellitero, S., Hernàndez, M., Del Castillo, D., Richart, C., 2013. Plasma visfatin levels and gene expression in morbidly obese women with associated fatty liver disease. Clin. Biochem. 46, 202e208.

Bendtsen, L.Q., Lorenzen, J.K., Gomes, S., Liaset, B., Holst, J.J., Ritz, C., Reitelseder, S., Sjodin, A., Astrup, A., 2014. Effects of hydrolysed casein, intact casein and intact whey protein on energy expenditure and appetite regulation: a randomised, controlled, cross-over study. Br. J. Nutr. 112, 1412e1422.

Blachier, M., Leleu, H., Peck-Radosavljevic, M., Valla, D.C., Roudot-Thoraval, F., 2013. The burden of liver disease in Europe: a review of available epidemiological data. J. Hepatol. 58, 593e608.

Canto, C., Houtkooper, R.H., Pirinen, E., Youn, D.Y., Oosterveer, M.H., Cen, Y., Fernandez-Marcos, P.J., Yamamoto, H., Andreux, P.A., Cettour-Rose, P., Gademann, K., Rinsch, C., Schoonjans, K., Sauve, A.A., Auwerx, J., 2012. The NAD(+) precursor nicotinamide riboside enhances oxidative metabolism and protects against high-fat diet induced obesity. Cell Metab. 15, 838e847.

Canto, C., Menzies, K., Auwerx, J., 2015. NAD(+) metabolism and the control of energy homeostasis - a balancing act between mitochondria and the nucleus. Cell Metab. 22, 31e53.

Choi, S.E., Fu, T., Seok, S., Kim, D.H., Yu, E., Lee, K.W., Kang, Y., Li, X., Kemper, B., Kemper, J.K., 2013. Elevated microRNA-34a in obesity reduces NAD+ levels and SIRT1 activity by directly targeting NAMPT. Aging Cell 12, 1062e1072.

Dahl, T.B., Haukeland, J.W., Yndestad, A., Ranheim, T., Gladhaug, I.P., Damås, J.K., Haaland, T., Løberg, E.M., Arntsen, B., Birkeland, K., Bjøro, K., Ulven, S.M., Konopski, Z., Nebb, H.I., Aukrust, P., Halvorsen, B., 2010. Intracellular nicotinamide phosphoribosyltransferase protects against hepatocyte apoptosis and is down-regulated in nonalcoholic fatty liver disease. J.Clinical Endocrinol. Metab. 95, 3039e3047.

Drew, J.E., Farquharson, A.J., Horgan, G.W., Williams, L.M., 2016. Tissue-specific regulation of sirtuin and nicotinamide adenine dinucleotide biosynthetic pathways identified in C57Bl/6 mice in response to high-fat feeding. J. Nutr. Biochem. 37, 20e29.

Du, J., Zhou, Y., Su, X., Yu, J.J., Khan, S., Jiang, H., Kim, J., Woo, J., Kim, J.H., Choi, B.H., He, B., Chen, W., Zhang, S., Cerione, R.A., Auwerx, J., Hao, Q., Lin, H., 2011. Sirt5 is a NAD-dependent protein lysine demalonylase and desuccinylase. Science 334, 806.

Du, Y., Cai, T., Li, T., Xue, P., Zhou, B., He, X., Wei, P., Liu, P., Yang, F., Wei, T., 2015. Lysine malonylation is elevated in type 2 diabetic mouse models and enriched in metabolic associated proteins. Mol. Cell. Proteomics 14, 227e236.

Dudzinska, W., Lubkowska, A., Dolegowska, B., Safranow, K., Jakubowska, K., 2010. Adenine, guanine and pyridine nucleotides in blood during physical exercise and restitution in healthy subjects. Eur. J. Appl. Physiol. 110, 1155e1162.

Ekstedt, M., Franzén, L., Mathiesen, U.L., Thorelius, L., Holmqvist, M., Bodemar, G., Kechagias, S., 2006. Long-term follow-up of patients with NAFLD and elevated liver enzymes. Hepatology 44, 865e873.

Fukuwatari, T., Shibata, K., 2013. Nutritional aspect of tryptophan metabolism. Int. J. Tryptophan Res. 6, 3e8.

Gariani, K., Menzies, K.J., Ryu, D., Wegner, C.J., Wang, X., Ropelle, E.R., Moullan, N., Zhang, H., Perino, A., Lemos, V., Kim, B., Park, Y.K., Piersigilli, A., Pham, T.X., Yang, Y., Ku, C.S., Koo, S.I., Fomitchova, A., Canto, C., Schoonjans, K., Sauve, A.A., Lee, J.Y., Auwerx, J., 2016. Eliciting the mitochondrial unfolded protein response by nicotinamide adenine dinucleotide repletion reverses fatty liver disease in mice. Hepatology 63, 1190e1204.

Gariani, K., Ryu, D., Menzies, K., Yi, H.S., Stein, S., Zhang, H., Perino, A., Lemos, V., Katsyuba, E., Jha, P., Vijgen, S., Rubbia-Brandt, L., Kim, Y.K., Kim, J.T., Kim, K.S., Shong, M., Schoonjans, K., Auwerx, J., 2017. Inhibiting poly-ADP ribosylation increases fatty acid oxidation and protects against fatty liver disease. J. Hepatol. 66, 132e141.

Gebhardt, R., 1992. Metabolic zonation of the liver: regulation and implications for liver function. Pharmacol. Therapeut. 53, 275e354.

Giblin, W., Skinner, M.E., Lombard, D.B., 2014. Sirtuins: guardians of mammalian healthspan. Trends Genet. 30, 271e286.

Go, Y., Jeong, J.Y., Jeoung, N.H., Jeon, J.H., Park, B.Y., Kang, H.J., Ha, C.M., Choi, Y.K., Lee, S.J., Ham, H.J., Kim, B.G., Park, K.G., Park, S.Y., Lee, C.H., Choi, C.S., Park, T.S., Lee, W.N.P., Harris, R.A., Lee, I.K., 2016. Inhibition of pyruvate dehydrogenase kinase 2 protects against hepatic steatosis through modulation of tricarboxylic acid cycle anaplerosis and ketogenesis. Diabetes 65, 2876.

Graeff, R., Lee, H.C., 2002. A novel cycling assay for nicotinic acid-adenine dinu- cleotide phosphate with nanomolar sensitivity. Biochem. J. 367, 163e168.

Hirschey, M.D., Shimazu, T., Jing, E., Grueter, C.A., Collins, A.M., Aouizerat, B., Stancakova, A., Goetzman, E., Lam, M.M., Schwer, B., Stevens, R.D., Muehlbauer, M.J., Kakar, S., Bass, N.M., Kuusisto, J., Laakso, M., Alt, F.W., Newgard, C.B., Farese Jr., R.V., Kahn, C.R., Verdin, E., 2011. SIRT3 deficiency and mitochondrial protein hyperacetylation accelerate the development of the metabolic syndrome. Mol Cell 44, 177e190.

Kanehisa, M., Furumichi, M., Tanabe, M., Sato, Y., Morishima, K., 2017. KEGG: new perspectives on genomes, pathways, diseases and drugs. Nucleic Acids Res. 45, D353eD361.

Kendrick, A.A., Choudhury, M., Rahman, S.M., McCurdy, C.E., Friederich, M., Van Hove, J.L.K., Watson, P.A., Birdsey, N., Bao, J., Gius, D., Sack, M.N., Jing, E., Kahn, C.R., Friedman, J.E., Jonscher, K.R., 2011. Fatty liver is associated with reduced SIRT3 activity and mitochondrial protein hyperacetylation. Biochem. J. 433, 505e514.

Kim, H.S., Xiao, C., Wang, R.H., Lahusen, T., Xu, X., Vassilopoulos, A., Vazquez-Ortiz, G., Jeong, W.I., Park, O., Ki, S.H., Gao, B., Deng, C.X., 2010. Hepatic-specific disruption of SIRT6 in mice results in fatty liver formation due to enhanced glycolysis and triglyceride synthesis. Cell Metab. 12, 224e236.

Kohsaka, A., Laposky, A.D., Ramsey, K.M., Estrada, C., Joshu, C., Kobayashi, Y., Turek, F.W., Bass, J., 2007. High-fat diet disrupts behavioral and molecular circadian rhythms in mice. Cell Metabol. 6, 414e421.

Kuhl, C., Tautenhahn, R., Böttcher, C., Larson, T.R., Neumann, S., 2012. CAMERA: an integrated strategy for compound spectra extraction and annotation of LC/MS data sets. Anal. Chem. 84, 283e289.

Lazo, M., Clark, J.M., 2008. The epidemiology of nonalcoholic fatty liver disease: a global perspective. Semin. Liver Dis. 28, 339e350.

Loomba, R., Sanyal, A.J., 2013. The global NAFLD epidemic. Nat. Rev. Gastroenterol. Hepatol. 10, 686e690.

MacBride, M.M., Navis, A., Dasari, A., Perez, A.V., 2017. Mild reproductive impact of a Y chromosome deletion on a C57BL/6J substrain. Mamm. Genome 28, 155e165.

Maiuolo, J., Oppedisano, F., Gratteri, S., Muscoli, C., Mollace, V., 2016. Regulation of uric acid metabolism and excretion. Int. J. Cardiol. 213, 8e14.

McPherson, S., Hardy, T., Henderson, E., Burt, A.D., Day, C.P., Anstee, Q.M., 2015. Evidence of NAFLD progression from steatosis to fibrosing-steatohepatitis using paired biopsies: implications for prognosis and clinical management. J. Hepatol 62, 1148e1155.

Mills, K.F., Yoshida, S., Stein, L.R., Grozio, A., Kubota, S., Sasaki, Y., Redpath, P., Migaud, M.E., Apte, R.S., Uchida, K., Yoshino, J., Imai, S.i., 2016. Long-Term Administration of Nicotinamide Mononucleotide Mitigates Age-Associated Physiological Decline in Mice. Cell Metabol. 24, 795e806.

Pais, R., Charlotte, F.d., Fedchuk, L., Bedossa, P., Lebray, P., Poynard, T., Ratziu, V., 2013. A systematic review of follow-up biopsies reveals disease progression in patients with non-alcoholic fatty liver. J. Hepatol. 59, 550e556.

Penke, M., Larsen, P.S., Schuster, S., Dall, M., Jensen, B.A., Gorski, T., Meusel, A., Richter, S., Vienberg, S.G., Treebak, J.T., Kiess, W., Garten, A., 2015. Hepatic NAD salvage pathway is enhanced in mice on a high-fat diet. Mol. Cell. Endocrinol. 412, 65e72.

Pfluger, P.T., Herranz, D., Velasco-Miguel, S., Serrano, M., Tschöp, M.H., 2008. Sirt1 protects against high-fat diet-induced metabolic damage. Proc. Natl. Acad. Sci. 105, 9793e9798.

Purushotham, A., Schug, T.T., Xu, Q., Surapureddi, S., Guo, X., Li, X., 2009. Hepato- cyte-specific deletion of SIRT1 alters fatty acid metabolism and results in he- patic steatosis and inflammation. Cell Metabol. 9, 327e338.

Ramsey, K.M., Yoshino, J., Brace, C.S., Abrassart, D., Kobayashi, Y., Marcheva, B., Hong, H.K., Chong, J.L., Buhr, E.D., Lee, C., Takahashi, J.S., Imai, S., Bass, J., 2009. Circadian clock feedback cycle through NAMPT-mediated NAD+ biosynthesis. Science 324, 651e654.

Ratajczak, J., Joffraud, M., Trammell, S.A.J., Ras, R., Canela, N., Boutant, M., Kulkarni, S.S., Rodrigues, M., Redpath, P., Migaud, M.E., Auwerx, J., Yanes, O., Brenner, C., Cantó, C., 2016. NRK1 controls nicotinamide mononucleotide and nicotinamide riboside metabolism in mammalian cells. Nat. Commun. 7, 13103. Saggerson, D., 2008. Malonyl-coa, a key signaling molecule in mammalian cells. Annu. Rev. Nutr. 28, 253e272.

Shah, K., Stufflebam, A., Hilton, T.N., Sinacore, D.R., Klein, S., Villareal, D.T., 2009. Diet and exercise interventions reduce intrahepatic fat content and improve insulin sensitivity in obese older adults. Obesity (Silver Spring) 17, 2162e2168.

Smith, C.A., O'Maille, G., Want, E.J., Qin, C., Trauger, S.A., Brandon, T.R., Custodio, D.E., Abagyan, R., Siuzdak, G., 2005. METLIN: a metabolite mass spectral database. Ther. Drug Monit. 27, 747e751.

Smith, C.A., Want, E.J., O'Maille, G., Abagyan, R., Siuzdak, G., 2006. XCMS: processing mass spectrometry data for metabolite profiling using nonlinear peak align- ment, matching, and identification. Anal. Chem. 78, 779e787.

Team, R.C., 2013. 2006. R-a Language and Environment for Statistical Computing. RFoundation for Statistical Computing. Vienna, Austria. ISBN3-900051-07-0. http://www.R-project.org.

Toye, A.A., Lippiat, J.D., Proks, P., Shimomura, K., Bentley, L., Hugill, A., Mijat, V., Goldsworthy, M., Moir, L., Haynes, A., Quarterman, J., Freeman, H.C., Ashcroft, F.M., Cox, R.D., 2005. A genetic and physiological study of impaired glucose homeostasis control in C57BL/6J mice. Diabetologia 48, 675e686.

Trammell, S.A.J., Weidemann, B.J., Chadda, A., Yorek, M.S., Holmes, A., Coppey, L.J., Obrosov, A., Kardon, R.H., Yorek, M.A., Brenner, C., 2016. Nicotinamide riboside opposes type 2 diabetes and neuropathy in mice. Sci. Rep. 6, 26933.

Uddin, G.M., Youngson, N.A., Doyle, B.M., Sinclair, D.A., Morris, M.J., 2017. Nicotin- amide mononucleotide (NMN) supplementation ameliorates the impact of maternal obesity in mice: comparison with exercise. Sci. Rep. 7, 15063.

Verdin, E., 2015. NAD+ in aging, metabolism, and neurodegeneration. Science 350, 1208e1213.

Wang, X., Zhang, Z.F., Zheng, G.H., Wang, A.M., Sun, C.H., Qin, S.P., Zhuang, J., Lu, J., Ma, D.F., Zheng, Y.L., 2017. The inhibitory effects of purple sweet potato color on hepatic inflammation is associated with restoration of NAD(+) levels and attenuation of NLRP3 inflammasome activation in high-fat-diet-treated mice. Molecules 22, 1315.

Williams, L.M., Campbell, F.M., Drew, J.E., Koch, C., Hoggard, N., Rees, W.D., Kamolrat, T., Thi, N.H., Steffensen, I.L., Gray, S.R., Tups, A., 2014. The develop- ment of diet-induced obesity and glucose intolerance in C57BL/6 mice on a high-fat diet consists of distinct phases. PLoS One 9, e106159.

Wishart, D.S., Jewison, T., Guo, A.C., Wilson, M., Knox, C., Liu, Y., Djoumbou, Y., Mandal, R., Aziat, F., Dong, E., Bouatra, S., Sinelnikov, I., Arndt, D., Xia, J., Liu, P., Yallou, F., Bjorndahl, T., Perez-Pineiro, R., Eisner, R., Allen, F., Neveu, V., Greiner, R., Scalbert, A., 2013. HMDB 3.0ethe human Metabolome database in 2013. Nucleic Acids Res. 41, D801eD807.

Wong, V.W., Wong, G.L., Choi, P.C., Chan, A.W., Li, M.K., Chan, H.Y., Chim, A.M., Yu, J., Sung, J.J., Chan, H.L., 2010. Disease progression of non-alcoholic fatty liver dis- ease: a prospective study with paired liver biopsies at 3 years. Gut 59, 969e974. Wood, J.G., Rogina, B., Lavu, S., Howitz, K., Helfand, S.L., Tatar, M., Sinclair, D., 2004. Sirtuin activators mimic caloric restriction and delay ageing in metazoans. Nature 430, 686e689.

Wu, T., Liu, Y.h., Fu, Y.c., Liu, X.m., Zhou, X.h, 2014. Direct evidence of sirtuin downregulation in the liver of non-alcoholic fatty liver disease patients. Ann. Clin. Lab. Sci. 44, 410e418.

Xia, J., Wishart, D.S., 2002. Using MetaboAnalyst 3.0 for Comprehensive Metab- olomics Data Analysis. Current Protocols in Bioinformatics. John Wiley & Sons, Inc.

Yilmaz, Y., 2012. Review article: is non-alcoholic fatty liver disease a spectrum, or are steatosis and non-alcoholic steatohepatitis distinct conditions? Aliment. Pharmacol. Ther. 36, 815e823.

Yoshino, J., Mills, K.F., Yoon, M.J., Imai, S.i., 2011. Nicotinamide mononucleotide, a key NAD(+) intermediate, treats the pathophysiology of diet- and age-induced diabetes in mice. Cell Metab. 14, 528e536.

Zhang, H., Ryu, D., Wu, Y., Gariani, K., Wang, X., Luan, P., D'Amico, D., Ropelle, E.R., Lutolf, M.P., Aebersold, R., Schoonjans, K., Menzies, K.J., Auwerx, J., 2016. NAD+ repletion improves mitochondrial and stem cell function and enhances life span in mice. Science 352, 1436e1443.

Zhang, Z.F., Fan, S.H., Zheng, Y.L., Lu, J., Wu, D.M., Shan, Q., Hu, B., 2014. Troxerutin improves hepatic lipid homeostasis by restoring NAD(+)-depletion-mediated dysfunction of lipin 1 signaling in high-fat diet-treated mice. Biochem. Phar- macol. 91, 74e86.

Zhou, C.C., Yang, X., Hua, X., Liu, J., Fan, M.B., Li, G.Q., Song, J., Xu, T.Y., Li, Z.Y., Guan, Y.F., Wang, P., Miao, C.Y., 2016. Hepatic NAD+ deficiency as a therapeutic target for non-alcoholic fatty liver disease in ageing. Br. J. Pharmacol. 173, 2352e2368.